Published in final edited form as:

Arch Biochem Biophys. 2016 July 1; 601: 97–104. doi:10.1016/j.abb.2016.03.011.

Enhanced troponin I binding explains the functional changes produced by the hypertrophic cardiomyopathy mutation A8V of cardiac troponin C

Henry G. Zot[a], **Javier E. Hasbun**[b], **Clara A. Michell**[c], **Maicon Landim-Vieira**[c], and **Jose R. Pinto**[c]

[a]Department of Biology, University of West Georgia, Carrollton GA 30118

[b]Department of Physics, University of West Georgia, Carrollton GA 30118

[c]Department of Biomedical Sciences, College of Medicine, Florida State University, Tallahassee, FL

Abstract

Higher affinity for TnI explains how troponin C (TnC) carrying a causative hypertrophic cardiomyopathy mutation, TnC^{A8V}, sensitizes muscle cells to Ca^{2+}. Muscle fibers reconstituted with TnC^{A8V} require ~2.3-fold less [Ca^{2+}] to achieve 50% maximum-tension compared to fibers reconstituted with wild-type TnC (TnC^{WT}). Binding measurements rule out a significant change in N-terminus Ca^{2+}-affinity of isolated TnC^{A8V}, and TnC^{A8V} binds the switch-peptide of troponin-I (TnI^{sp}) ~1.6-fold more strongly than TnC^{WT}; thus we model the TnC-TnI^{sp} interaction as competing with the TnI-actin interaction. Tension data are well-fit by a model constrained to conditions in which the affinity of TnC^{A8V} for TnI^{sp} is 1.5-1.7-fold higher than that of TnC^{WT} at all [Ca^{2+}]. Mean ATPase rates of reconstituted cardiac myofibrils is greater for TnC^{A8V} than TnC^{WT} at all [Ca^{2+}], with statistically significant differences in the means at higher [Ca^{2+}]. To probe TnC-TnI interaction in low Ca^{2+}, displacement of bis-ANS from TnI was monitored as a function of TnC. Whereas Ca^{2+}-TnC^{WT} displaces significantly more bis-ANS than Mg^{2+}-TnC^{WT}, Ca^{2+}-TnC^{A8V} displaces probe equivalently to Mg^{2+}-TnC^{A8V} and Ca^{2+}-TnC^{WT}, consistent with stronger Ca^{2+}-independent TnC^{A8V}-TnI^{sp}. A Matlab program for computing theoretical activation is reported. Our work suggests that contractility is constantly above normal in hearts made hypertrophic by TnC^{A8V}.

Keywords

troponin I binding; modeling; cardiac troponin C; hypertrophic cardiomyopathy; myofibrillar ATPase; fluorescence

Corresponding Author: Jose Renato Pinto, Ph.D., Department of Biomedical Sciences, College of Medicine, Florida State University, Room 1350-H, 1115 West Call Street, Tallahassee, FL, USA 32306-4300. Tel: (850) 645-0016. Fax: (850) 644-9399. jose.pinto@med.fsu.edu, Henry G. Zot, PhD., Department of Biology, University of West Georgia, Carrollton, GA 30118. Tel: (678) 839-4016. Fax: (678) 839-6548. hzot@westga.edu.

INTRODUCTION

Hypertrophic cardiomyopathy (HCM) is a disease of the myocardium in which the left ventricle wall becomes abnormally thick and stiff. Mutations in sarcomeric proteins have been reported as a primary source of dysfunction leading to the development of HCM in humans (1–5). Although sarcomeric protein mutations are considered "poison peptides" due to their negative impact on muscle regulation, little is known about the molecular mechanisms underlying changes in protein function. Within the sarcomere, *TNNC1* (gene encoding cardiac troponin C, TnC) is a target for mutations associated with HCM (6–10). Of the missense mutations of *TNNC1*, A8V, causes the largest increase in Ca^{2+}sensitivity of force development (7).

Cardiac troponin C function integrates with the exchange of Ca^{2+} within the cytosol. Aside from buffering Ca^{2+} in myocytes (11), TnC controls the kinetics of cardiac muscle activation and relaxation in response to association and dissociation of Ca^{2+} (12). As a component of myofibrils, TnC participates with the transport mechanisms of the sarcoplasmic reticulum and sarcolemma to regulate and respond to transient Ca^{2+} concentrations in the range of 10^{-7} to 10^{-5} M during rest and peak activation, respectively (13).

A divalent cation binding site (site II) in the N-terminal domain of TnC is specific for Ca^{2+} (14), which allows the N-terminal domain to exist in predominantly a ligand-free or ligand-bound form during resting or activating states, respectively (15). Ligand binding to site II is energetically coupled to an equilibrium of closed and open conformations of the N-terminal domain (16). Ca^{2+} binding destabilizes the secondary structure required for the closed conformation, thereby increasing the probability of the open conformation (17). The open conformation exposes a hydrophobic patch that interacts with H3(I) of cardiac troponin I (TnI) (Fig. 1). H3(I) together with H4(I) comprise a larger switch peptide (TnI^{sp}) (16,18) that, along with the C-terminal domain of TnI, stabilizes troponin (Tn) and tropomyosin (Tm) in the position that blocks activation during rest (19–21). To activate contraction, TnI^{sp} rotates away from actin to bind the open conformation of TnC (18). TnI^{sp} binds the hydrophobic patch during the time that the N-terminal domain of TnC is in the open state, by a conformational selection mechanism (22–24). Baseline and maximum activation reflect the distributions of closed and open conformations, which have probabilities that depend on Ca^{2+} binding.

Although force measurements suggest that the A8V mutation acts by increasing the Ca^{2+} binding to N-terminal of domain of TnC as the primary cause of the disease (7), structural and functional measurements do not support this mechanism. No significant difference in N-terminal domain Ca^{2+} affinity is observed between isolated TnC^{A8V} and wild-type (WT) TnC (TnC^{WT}) (25). Instead, the A8V mutation shifts the conformation of the N-terminal domain in favor of the open conformations of ligand- bound and ligand- free TnC (26). The A8V mutation is located in the N-helix of the crystal structure of TnC^{WT} and is situated between site II for Ca^{2+} and the H3(I) interaction site (Fig. 1) (18). A synthetic peptide corresponding to TnI^{SP} binds to TnC^{A8V} ~1.6-fold more strongly than to TnC^{WT} (27). Based on these observations, we hypothesize that altered interactions between TnC and

TnI^{SP} is the primary source of the changes in function observed for myofilaments carrying TnC^{A8V} (e.g., increase myofilament Ca^{2+} sensitivity). We present a model to reconcile this hypothesis with the paradoxical increased sensitivity to Ca^{2+} observed in force measurements (7).

MATERIALS AND METHODS

Three-dimensional Visualization

The location of the TnC^{A8V} mutation within the 52- kDa Tn complex was visualized in the 1J1E Protein Data Bank file using PyMol software. PyMol is an open source molecular visualization program that allows manipulation of PDB files containing molecular coordinates obtained from structures based on x-ray crystallography or nuclear magnetic resonance.

Proteins

Human TnC^{WT}, TnC^{A8V}, and TnI were recombinantly expressed and purified according to established protocols (25,28).

Myofibrillar preparation

Porcine cardiac myofibrils were prepared as described previously (29) and stored in 50% glycerol at −20°C. Glycerol was removed by centrifugation (7 min at 800 × *g* and 4°C), and myofibrils were resuspended in wash buffer (10 mM MOPS, 10 mM KCl, pH 7.0) with 2 mM DTT.

Protein extraction and reconstitution

Native TnC was depleted from myofibrils using a CDTA extraction buffer (5 mM CDTA, 5 mM DTT, pH 8.4) for ~2.5 h at room temperature. After each 30 min of incubation, the myofibrils were centrifuged (5 min at 750 × *g* and 4°C), the supernatant was discarded, and a new CDTA extraction solution was added. To remove CDTA, myofibrils were centrifuged (5 min at 1,500 × *g* and 4°C) and resuspended in wash buffer three times. Native TnC-extracted myofibrils were reconstituted with TnC^{WT} or TnC^{A8V} (1.0 mg/ml) for 1 h at 4°C. Non-specifically bound TnC was removed from the reconstituted samples by several washes (centrifugation and resuspension) using wash buffer. Myofibril concentrations were determined using a Pierce™ Coomassie Plus (Bradford) assay kit.

Myofibrillar ATPase activity

The ATPase assay was performed at various pCa values using solutions containing 2 mM EGTA, 3 mM NTA, 20 mM MOPS, 1 mM free Mg^{2+}, ~2.5 mM $MgATP^{2-}$, pH 7.0 with ionic strength fixed to 80 mM (adjusted with KCl) and selected Ca^{2+} concentrations. The free Ca^{2+} in the ATPase solutions were calculated using pCa calculator software (30). The pCa values of the solutions were 8.0, 7.0, 6.6, 5.8, and 5.0 (1.0×10^{-8} M, 1.0×10^{-7} M, 2.51×10^{-7} M, 1.58×10^{-6} M and 1.0×10^{-5} M free Ca^{+2}, respectively). The myofibrillar concentration was 0.4 mg/ml, and the experiments were carried out at 25°C. The reaction was initiated by adding ATP and quenched after 7 min with the addition of ~4.6%

trichloroacetic acid. The precipitated proteins were collected by centrifugation (7 min at 3,095 × *g* and 4°C). Inorganic phosphate released by ATP hydrolysis was measured in the supernatant using the colorimetric method of Fiske and Subbarow (31).

Fluorescence assay

TnC^{WT}, TnC^{A8V}, and TnI were dialyzed into fluorescence buffer containing 120 mM MOPS, 100 mM KCl, and 2 mM EGTA at pH 7.0. For experiments in the presence of Mg^{2+} and Ca^{2+}, $MgCl_2$ and $CaCl_2$ were added before titration to yield final concentrations of 2 mM free Mg^{2+} and 0.1 mM free Ca^{2+}. For experiments in the presence of Mg^{2+} only, $MgCl_2$ was added to a final concentration of 2 mM free Mg^{2+}. In addition, before titration, freshly prepared 1 mM DTT was added to the buffer. TnI and 4,4′-dianilino-1,1′- binaphthyl-5,5′-disulfonic acid, dipotassium salt (bis-ANS) were fixed at 0.5 mM. TnC^{WT} or TnC^{A8V} was titrated at every 0.05 μM until reaching 0.5 μM, followed by titration of every 0.1 μM until the final concentration of 1 μM was reached. TnC and TnI concentrations were determined by spectroscopy at 280 nm (NanoDrop ND-1000 spectrophotometer) with extension coefficients of 4,595 and 9,770 cm^{-1} M^{-1}, respectively. The steady-state fluorescence measurements were performed in a Jasco FP-8300 spectrofluorometer at a constant photomultiplier (PMT) voltage of 340 V. The fluorescent probe bis-ANS was excited at 390 nm, emission was detected in a wavelength range of 450–520 nm, and the highest peak intensity was recorded. The experiments were carried out at 25°C and under constant stirring (600 rpm). A baseline experiment was performed in the absence of TnI to measure the fluorescence changes upon binding of TnC to bis-ANS. At the PMT voltage of 340V, minimum changes in fluorescence emission (A.U.) were observed in the baseline titration. The data obtained were then subtracted from the baseline. Data were analyzed and fit using linear regression.

Statistical analyses

The data were analyzed for significance using Student's *t*-test (unpaired). The results were considered statistically different when $p < 0.05$. The data are expressed as means ± S.E.

RESULTS

Modeling

We model regulation as modulation of Tm in the activated state (*M*) by multiple equilibria (32). In this model, *M* forms in the activated position of the thin filament as a ternary complex of myosin, Tm, and actin (33,34) from Tm in the central position of the thin filament (*C*) by a spontaneous process (equilibrium pathway). The equilibrium is perturbed by the crossbridge cycle in the physiologic muscle by an additional kinetic pathway. The kinetic pathway operates continuously with fixed non-zero probability to regenerate *M* without sampling *C*. Failure to regenerate returns Tm to the central position. The kinetic pathway is responsible for establishing an ensemble of Tm molecules that function as a unit in the manner predicted by theory (32) and consistent with the observation that an initial binding of two myosin heads establishes a regulatory unit that can accommodate binding by a much larger number of secondarily bound myosin heads (35). The combination of

equilibrium and kinetic pathways are expressed in the model as $C \overset{K_0'}{\rightleftarrows} M$ (Fig. 2), where K_0' includes the number of Tm molecules functioning as an ensemble ($n > 1$). In addition, the odds of regenerating M without decay to C (α) is included in the mathematical expression of M,

$$M = K_0' C (1 + (\alpha - 1) M)^n \quad (1)$$

that is derived for the steady-state (36). C is the only Ca^{2+}-dependent variable of Eq. 1 with K_0', α, and n each having fixed values determined empirically from WT data (see Table 1).

Regulation is achieved by controlling the availability of C for M formation (Eq. 1). C is consumed in the reactions that transition Tm to the blocking position of the thin filament and form the interaction between actin and TnI^{SP} (B_i; Fig. 2), which is responsible for muscle relaxation. Expressed in mole fractions, $C = 1 - M - B_1 - B_2$.

The reaction $C_i \overset{K_j T_i}{\rightleftharpoons} B_i$ ($i = 1, 2$ and $j = 1, 3$; Fig. 2) represents two independent events required for transition to the blocking state (B_i), namely, thermal-elastic transfer of Tm from the central position to the blocking position, and interaction between actin and TnI^{sp}. Dissociation of TnI^{sp} and movement of Tm to either the central or activated positions chemically uncouples Tn from spontaneous interaction with actin. Letting T_i represent uncoupled Tn, mole fractions of coupled and uncoupled Tn are determined by the relation, $1 = B_1 + B_2 + T_1 + T_2$.

By detailed balance (Fig. 2), the following relationship must hold,

$$K_2/K_4 = K_1/K_3 > 1 \quad (2)$$

Analysis of tension data

Fibers reconstituted with TnC^{A8V} require less Ca^{2+} to achieve a given fraction of maximum tension than fibers reconstituted with TnC^{WT} (7). Because site II of TnC^{WT} and TnC^{A8V} have indistinguishable affinities for Ca^{2+} (25), enhanced sensitivity to Ca^{2+} is more likely explained by strengthened interaction between TnC and TnI^{sp}. We model no change in Ca^{2+} affinity by holding K_2 and K_4 constant and an increase in TnI^{sp} affinity as a reduction in the apparent affinity of TnI^{sp} for actin, i.e. reduction in K_1 and K_3 (Fig. 2). Holding K_2/K_4 constant implies that K_1/K_3 is constant (Eq. 2).

To vary only K_1 and keeping K_1/K_3 constant, values for the other parameters must be fixed in Eq. 1. For simplicity, K_0' is set to unity and n, and α have values used previously ((32); see also Table 1). Because K_2 governs the binding of Ca^{2+} to uncoupled Tn (Fig. 2), K_2 is set approximately equal to the measured affinity constant for isolated Tn, and, hence, K_4 is given by K_2K_3/K_1 (Eq. 2). We compare K_2 and K_1/K_3 values derived previously for skeletal muscle (32) with substantially greater values of each as a means of testing sensitivity (Table 1). For both lower and upper boundary conditions, parameter K_1 is adjusted to achieve

theoretical activations that fit Ca^{2+}-dependent tension data normalized between 0% and 100% maximum (Fig. 3A, B). A 1.5- to 1.7- fold decrease in the bench-mark K_1 shifts the theoretical Ca^{2+} activation curve to align with the tension data collected for fibers reconstituted with TnC^{A8V} (Fig. 3A, B). By Eq. 2 and the constraint imposed on K_2 and K_4, the model predicts that K_3 also must decrease 1.5- to 1.7- fold. Although a unique solution is not established, this analysis reconciles the shift observed in Ca^{2+} sensitive force (7) and the absence of measured change in Ca^{2+} binding affinity in isolated TnC (25). A Matlab program to reproduce and extend the modeling shown here is included in Supplementary Material (Fig. S1). As a control, we fit a 2- fold increase in Ca^{2+} activation data published for the L48Q mutation of TnC by holding K_1 constant and increasing K_2, consistent with the increase in affinity of Tn reported for this mutation (Supplementary Material, Fig. S2).

On an absolute scale, the predicted activation is greater for all Ca^{2+} concentration between baseline and maximum fractional activations of 0.1–0.9 and 0.05–0.95 for lower and upper boundary conditions, respectively (Fig 3C, D; Table 1). Based on the shift to the open conformation described for TnC^{A8V} (26), we interpret the decrease in both K_1 and K_3 as owing to increased competition for TnI^{SP} by the more probable open conformation of TnC^{A8V}. Hence, the model predicts that a modest increase in contractility at all Ca^{2+} concentrations causes the leftward shift in the relative force curve (Fig. 3A, B).

Activation of myofibrillar ATPase

To test the model's prediction on an absolute scale, we measured Ca^{2+}-dependent ATPase rate of cardiac myofibrils reconstituted with TnC^{A8V} and TnC^{WT}. Given midrange Ca^{2+} concentration, *i.e.*, pCa 5.8, ATPase rates of myofibrils reconstituted with TnC^{WT} and TnC^{A8V} are 48.7% and 62.5% of maximum, respectively (Table 2). This difference is consistent with the enhancement observed in the tension record (Fig. 3A). Given various Ca^{2+} concentrations, all conditions stimulated higher mean ATPase rates for myofibrils reconstituted with TnC^{A8V} than myofibrils reconstituted with TnC^{WT} (Fig. 4). Differences in the means are statistically significant for Ca^{2+} concentrations above the midrange (Table 2). Elevation in ATPase rate at the extremes of Ca^{2+} concentration is consistent with a general increase in contractility brought about by the interaction between the more open TnC^{A8V} and TnI conformations.

Titration of fluorescence associated with TnI

To detect subtle differences in the interaction between TnC and TnI, we monitored the fluorescence of bis-ANS. Compared with bis-ANS bound to TnI, unbound bis-ANS has much reduced fluorescence intensity. We interpret reduction in fluorescence intensity as owing to the displacement of bis-ANS that results from complex formation between TnC and TnI. Rather than a typical hyperbolic binding curve, we observe a linear decrease in fluorescence as a function of added TnC (Fig. 5). Specific binding of TnC is evident from the saturation of the fluorescence decrease for additions that exceed 1 mol TnC/mol TnI (Fig. 5 insets). The appearance of irreversible binding may be explained by a combination6 of high affinity mass action binding (37) and persistent weak interactions that slow the diffusive separation of unbound proteins. To distinguish between the functions of the domains of TnC, we conducted the assay in two Ca^{2+} concentrations. Letting Mg-TnC^{WT}

and Ca-TnC^{WT} represent the structures of TnC in low or saturating Ca^{2+} concentrations (see introduction), both structures are expected to form high-affinity interactions between the C-terminal domain of TnC and TnI. However, only Ca-TnC^{WT} is expected to promote a secondary interaction between the N-terminal domain of TnC and TnI. As expected, the more extensively bound Ca-TnC^{WT} displaces proportionately more bis-ANS than Mg-TnC^{WT} (Fig. 5A). By contrast, Ca-TnC^{A8V} and Mg-TnC^{A8V} displace nearly the same amount of probe (Fig. 5B) and have nearly the same slope as Ca-TnC^{WT}. Thus, compared with Mg-TnC^{WT}, the N-terminal domain of Mg-TnC^{A8V} appears to have a more stable association with TnI, consistent with having a more open N-terminal domain conformation independent of Ca^{2+}-binding at site II.

DISCUSSIONS

We find that a modest increase in affinity between the N-terminal domain of TnC and the switch region of TnI causes the observed shift in midrange tension output to lower Ca^{2+} concentration observed in cardiac muscle containing TnC^{A8V}. Evidence in support of this hypothesis comes from the combination of experimental and modeling approaches. Measurement of binding rules out a significant change in Ca^{2+} binding affinity, and structural modeling rules out mutagenesis directed to the site of interaction between TnC and TnI. Based on a kinetic model of muscle regulation, we determined that the observed enhancement in Ca^{2+}-sensitivity is explained by 1.5- to 1.7-fold greater affinity between TnC and TnI^{SP}, which matches the experimental measurement of 1.6 fold (27). Average myofibril ATPase rates are higher for myofibrils reconstituted with TnC^{A8V} at all Ca^{2+} concentrations tested, and are significantly higher for Ca^{2+} concentrations above the titration midpoint. Compared with TnC^{WT}, TnC^{A8V} displaced more fluorescent probe from TnI in the absence of saturating Ca^{2+}, consistent with a stronger interaction.

Our model is distinct in the manner by which Ca^{2+} participates in attaining the activated state. Standard models derived from Hill et al. (38) are fundamentally allosteric and hence propose structural changes in Tm owing to a series of structural changes initiated by Ca^{2+} binding to site II of TnC. Accordingly, the states of Tm corresponding to the B, C, and M positions result from Ca^{2+}-free and myosin unbound; Ca^{2+}-bound and myosin weakly bound to actin; and, Ca^{2+}-bound and myosin strongly bound to actin, respectively (39–41). In our model, Ca^{2+}-binding acts only to shift the equilibrium between closed and open states of TnC and TnI^{sp} selects the open conformation of TnC independent of cation occupancy of TnC site II. Competition for TnI^{sp} between actin and the open conformation of TnC occurs only in the B position. By moving to the C and M positions, Tm prevents the actin-TnI^{sp} interaction, but not the interaction between the open conformation of TnC and TnI^{sp}. In these uncoupled positions, TnI^{sp} binding stabilizes the open conformation and hence increases site II affinity for Ca^{2+}. We diagram a representative distribution of closed and open conformations of TnC for each Tn state to show how the competition by actin for TnI^{sp} in state *B* shifts the equilibrium most strongly in favor of the closed conformation of TnC and the lack of competition in state *T* shifts the equilibrium most strongly in favor of the open conformation of TnC (Fig. 2).

Whereas the activated states of allosteric models require contribution of binding by both Ca^{2+} and strong-binding crossbridges, the activated state of our model requires no direct participation of Ca^{2+} binding. Instead, the activated state requires only Tm in the C position and force-bearing cycling crossbridges, consistent with consensus observations (41). Cooperative activation (39) without direct participation of ligand, *i.e.*, non-allosteric cooperativity, is a hallmark of a second chance mechanism (36). The statistical basis of a second chance mechanism can be linked to fundamental thermodynamic properties of systems that couple equilibrium and kinetic forces, such as forces acting on Tm by cycling crossbridges (42). Absent experimental proof of a Ca^{2+}-driven conformation of Tm being required for the activated state of the physiologic muscle, the simplest explanation is that Ca^{2+} binding is required only to perturb the equilibrium of closed and open states of TnC.

To date, three distinct probands carrying the Ala8 to Val mutation in TnC have been reported ((7,43) and personal communication). Although one of the probands reported a parent who was also positively genotyped for the mutation, the available genetic data remain difficult to interpret. In one clinical report, the mutation arose *de novo*; in another report, the proband carried two mutations in different sarcomeric proteins (7,43). The functional characterization is crucial to ascertain whether the A8V mutation in TnC is a true pathogenic variant and how it exerts its negative effect on muscle regulation.

Functional assays conducted with reconstituted proteins have shown that when the A8V mutant TnC is incorporated in the thin filament, it increases Ca^{2+} sensitivity of the myofilament. Kinetic measurements in reconstituted thin filament have suggested that a slower Ca^{2+} off rate might be the cause of the increased Ca^{2+} binding affinity to the N-terminal domain of TnC^{A8V} (28,44). Activation and deactivation of muscle is controlled by Ca^{2+} binding and dissociating from the TnC N-terminal domain, which subsequently interacts with the C-terminal domain of TnI. Therefore, not only Ca^{2+} kinetics but also TnC and TnI affinity are crucial in the regulation of cardiac muscle contraction. Little is known about how TnC^{A8V} delays the Ca^{2+} off rate and whether this involves an abnormal interaction between TnC and TnI. One simplistic explanation supported by our model is that the N-terminal domain of TnC^{A8V} binds with greater affinity to the TnI C-terminal domain. The fluorescence binding studies reported here are in agreement with a previous report (27) and support the hypothesis that TnC^{A8V} and TnI bind to each other at a higher affinity during resting conditions, when the muscle should be fully relaxed.

The consequences of increased binding affinity between TnC^{A8V} and TnI may have broader physiological implications. The functional consequences of the A8V substitution in TnC were evaluated in a knock-in (KI) mouse (45). Intact cardiomyocytes isolated from both heterozygous and homozygous KI mice had slower sarcomere length relaxation time and Ca^{2+} decay at different frequencies of stimulation. Furthermore, homozygous mice showed signs of diastolic dysfunction and a hypercontractile phenotype, *e.g.*, increased ejection fraction (45). The *in vivo* data can be correlated with the myofibrillar ATPase findings since higher myofibrillar ATPase activation can indicate a greater degree of muscle activation. Increased actomyosin ATPase activation was also observed in an early report (44). Here, we observed increased mean myofibrillar ATPase activity at all low Ca^{2+} concentrations tested, although statistical significance could not be demonstrated for all Ca^{2+} concentrations,

reflecting sensitivity limits of the assay. We interpret an effect of the TnC-TnI interaction on myofibrillar ATPase as contributing to the contractility of cardiac myocytes. Hence, even a small but persistent increase in myofibrillar ATPase at low Ca^{2+} levels may be sufficient to cause hypertrophy of the muscle over time.

In conclusion, these results suggest that the effect of the A8V mutation in delaying the Ca^{2+} off rate from TnC would be secondary to altering the interaction between TnC and TnI. This is an important observation because new therapies could be tailored to specifically target binding between TnC and TnI, rather than intracellular Ca^{2+} concentration or Ca^{2+} binding to TnC. The results obtained in this work do not allow us to determine in exact nature of the altered interactions between TnC and TnI; however, if the defect lies in the kinetics of binding to TnI rather than dissociation from TnI, this could be an important site for the development of a therapeutic target.

Supplementary Material

Refer to Web version on PubMed Central for supplementary material.

ACKNOWLEDGEMENTS

J.R.P. acknowledges support from the National Heart, Lung, and Blood Institute (NIH) Grant HL103840, Florida Heart Research Institute, and American Heart Association (AHA) 15GRNT25280004. We thank Dr. Anita Zot for expert editing assistance during revision.

ABBREVIATIONS

TnC	Cardiac troponin C
TnI	Cardiac troponin I
Tm	Cardiac tropomyosin
Tn	Cardiac troponin
A8V	Alanine to valine replacement at position 8 of cardiac troponin C
TnI^{sp}	Switch peptide of cardiac TnI
HCM	Hypertrophic cardiomyopathy
***TNNC*1**	Gene encoding cardiac troponin C
CDTA	1,2-Diaminocyclohexanetetraacetic acid disodium
DTT	Dithiothreitol
EGTA	Ethylene glycol-bis(2-aminoethylether)-*N,N,N′,N′*-tetraacetic acid
NTA	Nitrilotriacetic acid

MOPS	3-(N-Morpholino)propanesulfonic acid, 4-Morpholinepropanesulfonic acid
ATP	Adenosine 5′-triphosphate
Bis-ANS	4,4′-Dianilino-1,1′-Binaphthyl-5,5′-Disulfonic Acid, Dipotassium Salt
pCa	$10^{-[Ca2+]}$

REFERENCES

1. Konno T, Chang S, Seidman JG, Seidman CE. Genetics of hypertrophic cardiomyopathy. Current opinion in cardiology. 2010; 25:205–209. [PubMed: 20124998]
2. Marian AJ. Hypertrophic cardiomyopathy: from genetics to treatment. European journal of clinical investigation. 2010; 40:360–369. [PubMed: 20503496]
3. Willott RH, Gomes AV, Chang AN, Parvatiyar MS, Pinto JR, Potter JD. Mutations in Troponin that cause HCM, DCM AND RCM: what can we learn about thin filament function? Journal of molecular and cellular cardiology. 2010; 48:882–892. [PubMed: 19914256]
4. Force T, Bonow RO, Houser SR, Solaro RJ, Hershberger RE, Adhikari B, Anderson ME, Boineau R, Byrne BJ, Cappola TP, Kalluri R, LeWinter MM, Maron MS, Molkentin JD, Ommen SR, Regnier M, Tang WH, Tian R, Konstam MA, Maron BJ, Seidman CE. Research priorities in hypertrophic cardiomyopathy: report of a Working Group of the National Heart, Lung, and Blood Institute. Circulation. 2010; 122:1130–1133. [PubMed: 20837938]
5. Maron BJ, Maron MS. Hypertrophic cardiomyopathy. Lancet. 2013; 381:242–255. [PubMed: 22874472]
6. Hoffmann B, Schmidt-Traub H, Perrot A, Osterziel KJ, Gessner R. First mutation in cardiac troponin C, L29Q, in a patient with hypertrophic cardiomyopathy. Hum Mutat. 2001; 17:524. [PubMed: 11385718]
7. Landstrom AP, Parvatiyar MS, Pinto JR, Marquardt ML, Bos JM, Tester DJ, Ommen SR, Potter JD, Ackerman MJ. Molecular and functional characterization of novel hypertrophic cardiomyopathy susceptibility mutations in TNNC1-encoded troponin C. Journal of molecular and cellular cardiology. 2008; 45:281–288. [PubMed: 18572189]
8. Chung WK, Kitner C, Maron BJ. Novel frameshift mutation in Troponin C (TNNC1) associated with hypertrophic cardiomyopathy and sudden death. Cardiology in the young. 2011; 21:345–348. [PubMed: 21262074]
9. Parvatiyar MS, Landstrom AP, Figueiredo-Freitas C, Potter JD, Ackerman MJ, Pinto JR. A Mutation in TNNC1-encoded Cardiac Troponin C, TNNC1-A31S, Predisposes to Hypertrophic Cardiomyopathy and Ventricular Fibrillation. The Journal of biological chemistry. 2012; 287:31845–31855. [PubMed: 22815480]
10. Kalyva A, Parthenakis FI, Marketou ME, Kontaraki JE, Vardas PE. Biochemical characterisation of Troponin C mutations causing hypertrophic and dilated cardiomyopathies. J Muscle Res Cell Motil. 2014; 35:161–178. [PubMed: 24744096]
11. Bers, DM. Calcium sources and sinks. 2nd ed. Kluwer Academic Publishers; Boston/London: 2001.
12. Biesiadecki BJ, Davis JP, Ziolo MT, Janssen PM. Tri-modal regulation of cardiac muscle relaxation; intracellular calcium decline, thin filament deactivation, and cross-bridge cycling kinetics. Biophysical reviews. 2014; 6:273–289. [PubMed: 25484996]
13. Bers DM. Calcium fluxes involved in control of cardiac myocyte contraction. Circulation research. 2000; 87:275–281. [PubMed: 10948060]
14. Holroyde MJ, Robertson SP, Johnson JD, Solaro RJ, Potter JD. The calcium and magnesium binding sites on cardiac troponin and their role in the regulation of myofibrillar adenosine triphosphatase. The Journal of biological chemistry. 1980; 255:11688–11693. [PubMed: 6449512]

15. Davis JP, Tikunova SB. Ca(2+) exchange with troponin C and cardiac muscle dynamics. Cardiovascular research. 2008; 77:619–626. [PubMed: 18079104]
16. Gagne SM, Tsuda S, Li MX, Smillie LB, Sykes BD. Structures of the troponin C regulatory domains in the apo and calcium-saturated states. Nature structural biology. 1995; 2:784–789. [PubMed: 7552750]
17. Vinogradova MV, Stone DB, Malanina GG, Karatzaferi C, Cooke R, Mendelson RA, Fletterick RJ. Ca^{2+}-regulated structural changes in troponin. Proceedings of the National Academy of Sciences of the United States of America. 2005; 102:5038–5043. [PubMed: 15784741]
18. Takeda S, Yamashita A, Maeda K, Maeda Y. Structure of the core domain of human cardiac troponin in the Ca(2+)-saturated form. Nature. 2003; 424:35–41. [PubMed: 12840750]
19. Li MX, Spyracopoulos L, Beier N, Putkey JA, Sykes BD. Interaction of cardiac troponin C with Ca(2+) sensitizer EMD 57033 and cardiac troponin I inhibitory peptide. Biochemistry. 2000; 39:8782–8790. [PubMed: 10913289]
20. Luo Y, Wu JL, Li B, Langsetmo K, Gergely J, Tao T. Photocrosslinking of benzophenone-labeled single cysteine troponin I mutants to other thin filament proteins. Journal of molecular biology. 2000; 296:899–910. [PubMed: 10677290]
21. Tripet B, Van Eyk JE, Hodges RS. Mapping of a second actin-tropomyosin and a second troponin C binding site within the C terminus of troponin I, and their importance in the Ca2+-dependent regulation of muscle contraction. Journal of molecular biology. 1997; 271:728–750. [PubMed: 9299323]
22. Paakkonen K, Annila A, Sorsa T, Pollesello P, Tilgmann C, Kilpelainen I, Karisola P, Ulmanen I, Drakenberg T. Solution structure and main chain dynamics of the regulatory domain (Residues 1–91) of human cardiac troponin C. The Journal of biological chemistry. 1998; 273:15633–15638. [PubMed: 9624156]
23. Paakkonen K, Sorsa T, Drakenberg T, Pollesello P, Tilgmann C, Permi P, Heikkinen S, Kilpelainen I, Annila A. Conformations of the regulatory domain of cardiac troponin C examined by residual dipolar couplings. European journal of biochemistry / FEBS. 2000; 267:6665–6672. [PubMed: 11054120]
24. Gaponenko V, Abusamhadneh E, Abbott MB, Finley N, Gasmi-Seabrook G, Solaro RJ, Rance M, Rosevear PR. Effects of troponin I phosphorylation on conformational exchange in the regulatory domain of cardiac troponin C. The Journal of biological chemistry. 1999; 274:16681–16684. [PubMed: 10358006]
25. Pinto JR, Parvatiyar MS, Jones MA, Liang J, Ackerman MJ, Potter JD. A functional and structural study of troponin C mutations related to hypertrophic cardiomyopathy. The Journal of biological chemistry. 2009; 284:19090–19100. [PubMed: 19439414]
26. Cordina NM, Liew CK, Gell DA, Fajer PG, Mackay JP, Brown LJ. Effects of calcium binding and the hypertrophic cardiomyopathy A8V mutation on the dynamic equilibrium between closed and open conformations of the regulatory N-domain of isolated cardiac troponin C. Biochemistry. 2013; 52:1950–1962. [PubMed: 23425245]
27. Swindle N, Tikunova SB. Hypertrophic cardiomyopathy-linked mutation D145E drastically alters calcium binding by the C-domain of cardiac troponin C. Biochemistry. 2010; 49:4813–4820. [PubMed: 20459070]
28. Pinto JR, Reynaldo DP, Parvatiyar MS, Dweck D, Liang J, Jones MA, Sorenson MM, Potter JD. Strong cross-bridges potentiate the Ca(2+) affinity changes produced by hypertrophic cardiomyopathy cardiac troponin C mutants in myofilaments: a fast kinetic approach. The Journal of biological chemistry. 2011; 286:1005–1013. [PubMed: 21056975]
29. Solaro RJ, Pang DC, Briggs FN. The purification of cardiac myofibrils with Triton X-100. Biochimica et biophysica acta. 1971; 245:259–262. [PubMed: 4332100]
30. Dweck D, Reyes-Alfonso A Jr. Potter JD. Expanding the range of free calcium regulation in biological solutions. Anal Biochem. 2005; 347:303–315. [PubMed: 16289079]
31. Fiske CH, Subbarow Y. The colorimetric determination of phosphorous. Journal of Biological Chemistry. 1925; 66:375–400.
32. Zot HG, Hasbun JE, Van Minh N. Striated muscle regulation of isometric tension by multiple equilibria. PloS one. 2009; 4:e8052. [PubMed: 19997610]

33. Eaton BL. Tropomyosin binding to F-actin induced by myosin heads. Science. 1976; 192:1337–1339. [PubMed: 131972]
34. Tobacman LS, Butters CA. A new model of cooperative myosin-thin filament binding. The Journal of biological chemistry. 2000; 275:27587–27593. [PubMed: 10864931]
35. Desai R, Geeves MA, Kad NM. Using fluorescent myosin to directly visualize cooperative activation of thin filaments. The Journal of biological chemistry. 2015; 290:1915–1925. [PubMed: 25429108]
36. Zot HG, Hasbun JE, Minh NV. Second-chance signal transduction explains cooperative flagellar switching. PloS one. 2012; 7:e41098. [PubMed: 22844429]
37. Calvert MJ, Ward DG, Trayer HR, Trayer IP. The importance of the carboxyl-terminal domain of cardiac troponin C in Ca2+-sensitive muscle regulation. The Journal of biological chemistry. 2000; 275:32508–32515. [PubMed: 10921926]
38. Hill TL, Eisenberg E, Greene L. Theoretical model for the cooperative equilibrium binding of myosin subfragment 1 to the actin-troponin-tropomyosin complex. Proceedings of the National Academy of Sciences of the United States of America. 1980; 77:3186–3190. [PubMed: 10627230]
39. McKillop DF, Geeves MA. Regulation of the interaction between actin and myosin subfragment 1: evidence for three states of the thin filament. Biophysical journal. 1993; 65:693–701. [PubMed: 8218897]
40. Lehman W, Hatch V, Korman V, Rosol M, Thomas L, Maytum R, Geeves MA, Van Eyk JE, Tobacman LS, Craig R. Tropomyosin and actin isoforms modulate the localization of tropomyosin strands on actin filaments. Journal of molecular biology. 2000; 302:593–606. [PubMed: 10986121]
41. Manning EP, Tardiff JC, Schwartz SD. A model of calcium activation of the cardiac thin filament. Biochemistry. 2011; 50:7405–7413. [PubMed: 21797264]
42. Zot, HG.; Hasbun, JE.; Van Mihn, N. Common Basis for Cellular Motility. ArXiv Doc. 2015. arxiv.org/abs/1511.00123
43. Jaafar N, Girolami F, Zairi I, Kraiem S, Hammami M, Olivotto I. Genetic profile of hypertrophic cardiomyopathy in Tunisia: Is it different? Global Cardiology Science and Practice. 2015; 2015:16. [PubMed: 26779504]
44. Albury AN, Swindle N, Swartz DR, Tikunova SB. Effect of hypertrophic cardiomyopathy-linked troponin C mutations on the response of reconstituted thin filaments to calcium upon troponin I phosphorylation. Biochemistry. 2012; 51:3614–3621. [PubMed: 22489623]
45. Martins AS, Parvatiyar MS, Feng HZ, Bos JM, Gonzalez-Martinez D, Vukmirovic M, Turna RS, Sanchez-Gonzalez MA, Badger CD, Zorio DA, Singh RK, Wang Y, Jin JP, Ackerman MJ, Pinto JR. In Vivo Analysis of Troponin C Knock-In (A8V) Mice: Evidence that TNNC1 Is a Hypertrophic Cardiomyopathy Susceptibility Gene. Circulation. Cardiovascular genetics. 2015; 8:653–664. [PubMed: 26304555]

Highlights

1) TnC^{A8V} increases Ca^{2+}-dependent tension without altering N-domain Ca^{2+}-binding affinity in isolated protein

2) TnC^{A8V} enhances myofibrillar ATPase rates and TnI-TnC interaction

3) Theoretical predictions of enhanced TnI-TnC interaction recapitulate experimental published data

4) Stronger TnI-TnC^{A8V} interaction may destabilizes blocking caused by TnI-actin interaction

5) Permanent increase in contractility is the presumptive cause of hypertrophic cardiomyopathy

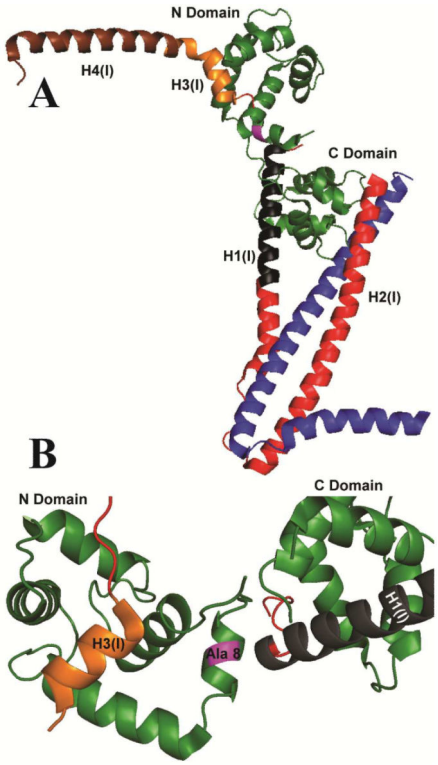

Figure 1. Ribbon diagram of the Ca^{2+}-saturated structure of cardiac Tn showing the site of the mutation (magenta)

A. Peptide backbones are shown for TnC (green), TnI (red, black, gold and brown) and TnT (blue). Residues 150–159 corresponding to the switch region of TnI, H3(I), are shown (gold) at the site of interaction with the hydrophobic patch of TnC. B. The position of alanine 8 (purple) is shown in relation to the H3(I) helix and the lobes of TnC, which form Ca^{2+}-dependent (N-Domain) and Ca^{2+}-independent (C-Domain) contacts with TnI.

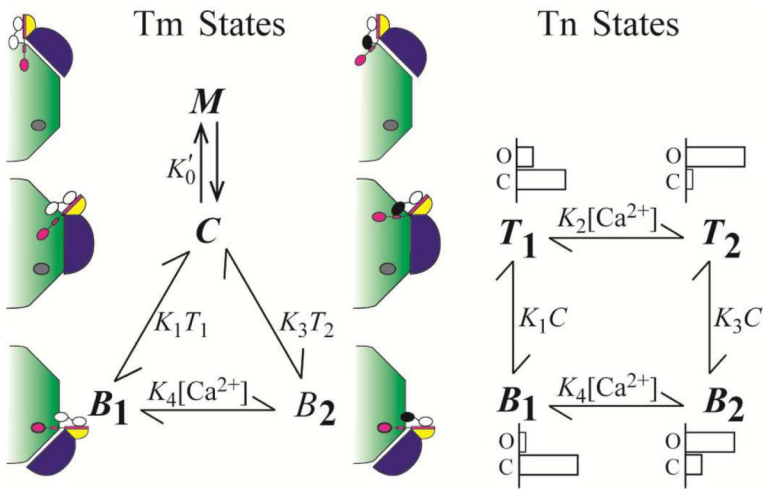

Figure 2. Model accounting for results of functional studies

The TnI^{sp} is modeled as binding either TnC or actin and TnC is modeled as being in either the closed or open conformation. The model consists of two subsystems that partially overlap. The states of Tm (blue) include *C*, *M*, and B_i ($i = 1, 2$), corresponding to interactions with actin (green) in positions central, myosin dependent, and blocking, respectively. Steady-state constant, K_0', governs the ensemble dynamic interactions of myosin with Tm that sustain *M*. The states of Tn (TnT, yellow; TnI, magenta, TnC, black-white) include T_i and B_i, corresponding to energetically coupled and uncoupled in the Ca^{2+}-free state ($i = 1$) and Ca^{2+}-bound state ($i = 2$), respectively. Most probable occupancy of the N-terminal domain regulatory site of TnC is shown as Ca^{2+}-bound (black) or Ca^{2+}-free (white). Equilibrium constants govern spontaneous interactions that occur between Tn and actin (K_1 and K_3), and Ca^{2+} and Tn (K_2 and K_4); K_1 and K_3 also include the equilibrium that favors Tm in the C position. For the Tn states, representative distributions of closed and open conformations of TnC are diagramed to show the ratios 9/1, 1/3, 3/1, and 1/9 for B_1, B_2, T_1, T_2, respectively, which are intended for relative comparison only.

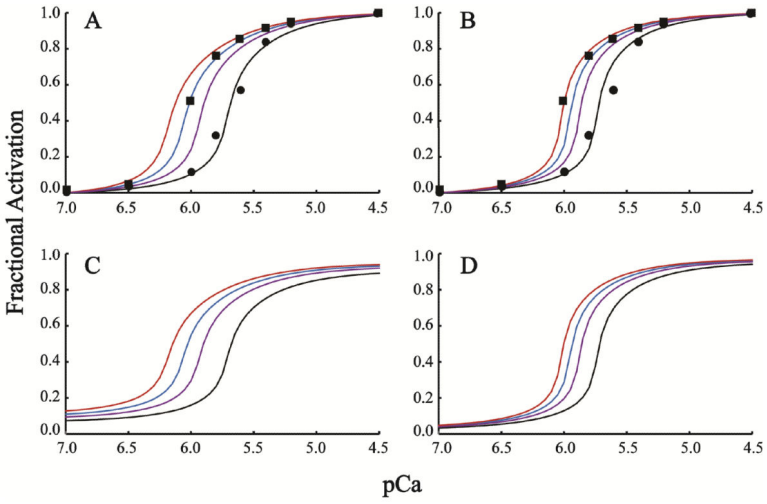

Figure 3. Tension data fit with model

Data from chemically skinned and TnC-depleted cardiac fibers are reproduced from an earlier study (7) for TnC^{WT} (circles) or TnC^{A8V} (squares). Normalized theoretical curves are shown for the fit of WT data (black) and for varying one parameter, K_1, by a multiplier (ΔK_1; Table 1), where $1/\Delta K_1$ is 1.3, 1.5, and 1.7 (purple, blue, red). A and B. Lower and upper K2 boundary conditions (Table 1) are plotted respectively on normalized scales. C and D. Theoretical curves from A and B shown on absolute scales.

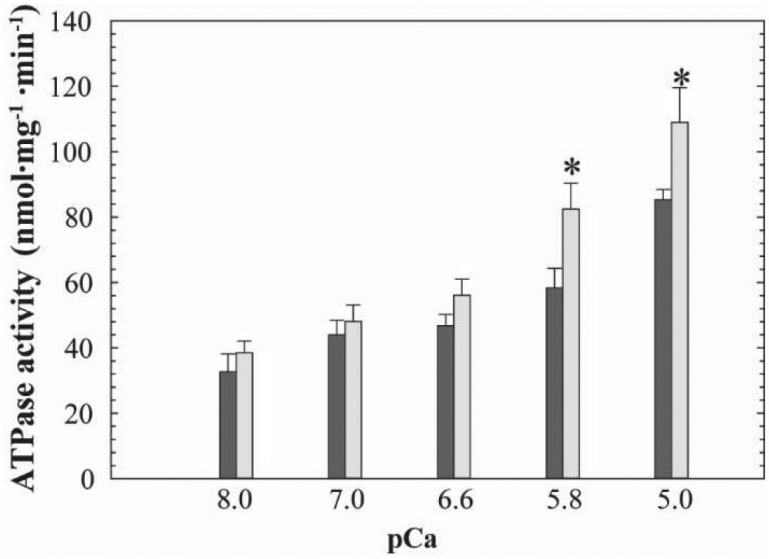

Figure 4. Ca^{2+}-dependent ATPase measurement of reconstituted TnC-depleted myofibrils

Myofibrils were reconstituted with TnC^{WT} (black) and TnC^{A8V} (gray). Mean ± SEM; n = 9. *p < 0.05 vs WT at same pCa. The specific ATPase activity measured in native cardiac myofibrils were 5.56 ± 2.06 and 55.15 ± 3.27 nmol Pi/mg/min at pCa 8.0 and pCa 5.0 (n = 7), respectively. The specific ATPase activity measured in TnC-extracted myofibrils were 12.03 ± 1.02 and 25.54 ± 2.65 nmol Pi/mg/min at pCa 8.0 and pCa 5.0 (n = 12), respectively.

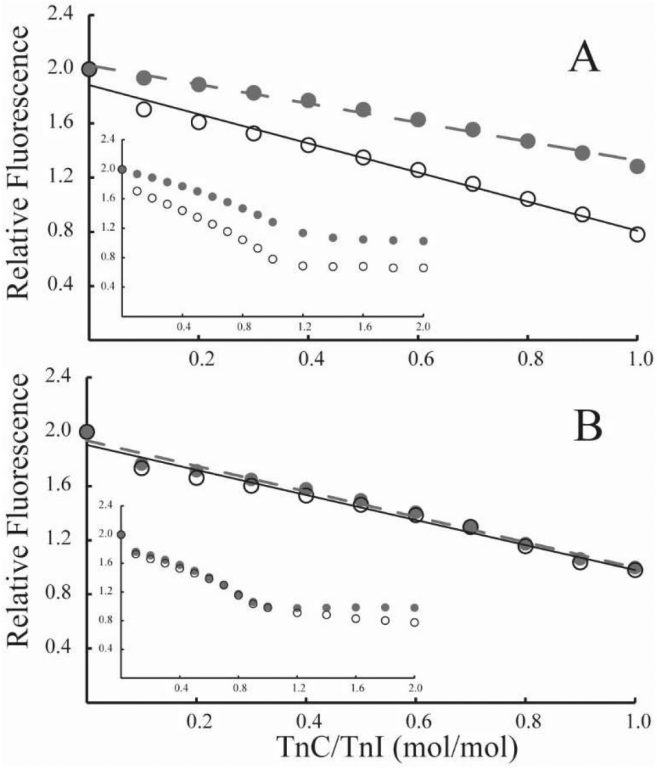

Figure 5. TnC titration of bis-ANS fluorescence associated with TnI

Plotted are titration of fluorescence change (arbitrary units) curves for TnC^{WT} (A) and TnC^{A8V} (B) with Ca^{2+} added (solid) or not added (open). Mean ± SEM; n = 4. Titrations are biphasic (insets) with the linear change saturating at 1 mol/mol TnC added. In A. linear regression of slopes corresponding to Ca^{2+}-bound (solid line) and Ca^{2+}-free (dashed line) are −1075 and −703, respectively. In B. linear regression of slopes corresponding to Ca^{2+}-bound (solid line) and Ca^{2+} free (dashed line) are −922 and −937, respectively.

Table 1

Summary of Model Specific Constants

	Lower K_2 Boundary[1]				Upper K_2 Boundary			
	WT	**A8V**	**A8V**	**A8V**	**WT**	**A8V**	**A8V**	**A8V**
ΔK_1 (note[2])		0.77	0.67	0.59		0.77	0.67	0.59
K_0'	1	1	1	1	1	1	1	1
[3] α	3.25	3.25	3.25	3.25	3.25	3.25	3.25	3.25
n	5	5	5	5	5	5	5	5
K_1	275.00	211.54	183.33	161.76	1400.00	1076.92	933.33	823.53
K_2 (note[3])	1.67	1.67	1.67	1.67	10.00	10.00	10.00	10.00
K_3 (note[4])	27.55	21.19	18.37	16.21	14.00	10.77	9.33	8.24
K_4	0.17	0.17	0.17	0.17	0.10	0.10	0.10	0.10
Range of Activation	~10% to- 90%	~10% to- 90%	~10% to- 90%	~10% to- 90%	~5% to- 95%	~5% to- 95%	~5% to- 95%	~5% to- 95%
Figures	3A, 3C	3A, 3C	3A, 3C	3A, 3C	3B, 3D	3B, 3D	3B, 3D	3B, 3D
Curve	Black	Red	Blue	Purple	Black	Red	Blue	Purple

[1] K_2, K_4, n, and α have values used previously (32). Values are dimensionless unless otherwise indicated.

[2] Multiplier of WT K_1

[3] Multiple of 10^6 M^{-1}

[4] Not an adjustable parameter. Tabulated value calculated from K_1K_4/K_2

Table 2

Summary of Cardiac Myofibrillar ATPase Activity

	TnC-WT	TnC-A8V
Cardiac Myofibrils	nmol Pi·mg^{-1}·min^{-1}	
pCa 8.0	32.65 ± 5.48	38.51 ± 3.55
pCa 7.0	44.01 ± 4.51	48.06 ± 5.07
pCa 6.6	46.79 ± 3.42	56.11 ± 4.90
pCa 5.8	58.29 ± 6.07	82.52 ± 7.85 *
pCa 5.0	85.25 ± 3.22	108.96 ± 10.65 *
	Ratios	
(pCa 5.8–8.0) / (pCa 5.0–8.0) × 100	48.7%	62.5%

* $p < 0.05$ *vs* WT